THE JOURNAL OF PHYSICAL CHEMISTRY A

Article

Cite This: J. Phys. Chem. A 2019, 123, 5683−5691

pubs.acs.org/JPCA

# Structure Distribution of Gaseous Ions in Strong Electrostatic Fields

Iraklis Litinas and Andreas D. Koutselos*

Department of Chemistry, Physical Chemistry Laboratory, National and Kapodistrian University of Athens, Panepistimiopolis, 15771 Athens, Greece

**ABSTRACT:** In drift tube experiments, where ions move in gases under the action of an electrostatic field, collision excitation is implemented for the study of the energy partitioning in the molecular degrees of freedom and the corresponding relaxation rates when the excitation is turned off. In the case of flexible ions, the vibration modes related to metastable molecular structures have been activated in ion mobility spectrometry and their population has been probed with respect to the field strength and the gas temperature. Here, we study the angular vibrational excitation and relaxation of such systems by examining the motion of molecular ions with one bending mode at strong fields using a nonequilibrium molecular dynamics simulation method. The relatively stable structures are introduced through the use of an intramolecular angular potential with minima at the position of the most stable conformations. We calculate the first few moments of the velocity and angular velocity distribution functions as well as the distribution of the conformers, and find that they follow unified curves when plotted with respect to the relative ion−atom collision energy. At high field strengths, the angular vibration is excited and a portion of the ions interchanges conformations continuously in time with the populations of the molecular structures to attain limiting values. In addition, orientational alignment, with the perpendicular angular momentum being greater than the one parallel to the field, is observed. Our observations, although based on a specific system, must be rather general for the case of large flexible molecular ions.

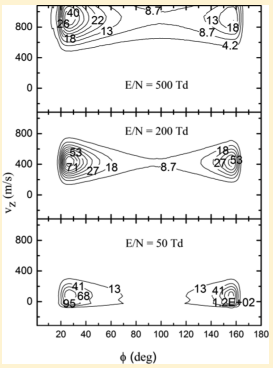




## 1. INTRODUCTION

The motion of ions in low-density gases at high electrostatic fields has been studied primarily in drift tube experiments. Various effects emerge due to the nonequilibrium nature of the state of the ions, starting from the growth of the third and fourth velocity moments, to the orientation alignment as the field increases,[1,2] the differentiation of the diffusion parallel and perpendicular to the field,[3] and velocity correlations that grow at short times.[4] Recently, the distribution of relatively stable structures of flexible ions has been probed at strong fields through ion mobility spectrometry (IMS) measurements,[5−9] and therefore its form and field dependence need to be studied. At rather short drift regions, the experimentalists have employed collision excitation with the use of different electric voltages to transform initially selected ion structures to other relatively stable isomers. In an IMS−IMS experimental arrangement[10] at weak fields, the measured populations of the ion structures are found to depend on the initial conformations, although at strong fields they are maintained at certain values irrespective of the initial conditions.

The field dependence of the abundance of the structures at high field strengths occurs at relaxed nonequilibrium states of the ions. As the ions are pulled by the electric field through a low-density gas, they accumulate energy due to collision excitation with the gas molecules and relax to a quasi-steady state. The gas, in turn, being in excess, extracts energy continuously from the ions, and remains always in equilibrium. In partial excitation at weak fields, depending on the intensity and the duration of the excitation, the molecular ion isomers are trapped in intramolecular potential energy minima, which are separated by energy barriers. These are overcome at strong fields when ions are excited through energetic collisions with the neutral gas leading to a modification of the population of the ion structures. The electric field thresholds, above which structure transformations emerge, have been related to relevant energy barriers and have been used for their estimation.[11,12]

To study the population of structures of flexible ions as well as their transport in gases under the action of strong electric fields, we employ a nonequilibrium molecular dynamics (MD) method[13] and a model flexible ion that resembles the BIP (*N*-*n*-butyl-2-(*β*-ionylidene)-4-methylpyridinium) ion, which has been studied through an IMS−IMS analytic procedure.[10] In this case, the ion conformers are selected from the first IMS procedure, subsequently excited through collision with neutral gas molecules at a range of electric field strengths in the middle section, and finally detected through the second IMS procedure. The excitation takes place in a narrow region (3 mm length) with a range of $E/N$ values of the ratio of the field strength to the gas density, from about 40 to 500 Td (1 Td = $10^{21}$ Vm$^2$), and a gas temperature of around 300 K. Since at weak fields the measured relative abundance of the structures was found to depend on the field strength and the initial (selected) molecular structure, it is apparent that the ions travel through the excitation region without having time to relax to a steady state. Only at strong fields, the relative populations appear to be independent of the field strength and the selected initial isomer.

**Received:** April 12, 2019
**Revised:** June 3, 2019
**Published:** June 4, 2019




DOI: 10.1021/acs.jpca.9b03441
J. Phys. Chem. A 2019, 123, 5683−5691

Since similar structure transformations of large molecular ions have also been observed through collisional excitation at a high gas temperature at weak fields,[6,14] it is interesting to identify similarities and possible differences between these two modes of excitation and relaxation, especially since the ion transport alone presents differences at weak and strong fields. For example, at high field values, the mean ion translational and rotational motions deviate from those of equilibrium and, in addition, orientation alignment and differences in the ion random energy parallel and perpendicular to the field are observed. In this case, the analytic solution of the kinetic theory applied for the ion motion has furnished an effective temperature parameter, $T_{eff}$, which describes the random ion energy and characterizes the ion transport properties as follows[15]

$$\frac{3}{2}kT_{eff} = \frac{3}{2}kT + \frac{1}{2}Mv_d^2(1+\beta) \quad (1)$$

where $T$ and $M$ are the temperature and mass of the gas, $v_d$ is the ion drift velocity, and $\beta$ is a parameter that contributes at high fields. This expression combines the (random) thermal energy of equilibrium (and of the gas) with an additional random energy contribution accumulated to the ion due to the action of the field. At weak fields ($\beta = 0$), the random energy reduces to the Wannier expression[16] for the relative ion-neutral kinetic energy, $E_w$, which characterizes conveniently the ion mobility close to equilibrium, $E_w = \frac{3}{2}kT + \frac{1}{2}Mv_d^2$. Here, we will be able to examine the possibility for the internal energy and the distribution of molecular structures of the ion to be described by the relative collision energy, expressed also through an effective temperature $T_w = 2E_w/3k$ at strong electric fields.

The transformation of the ion structures will be followed in the present MD simulation through the monitoring of the angle of the folding molecular structure that evolves in time under the influence of an intramolecular potential that has minima at the angles of the locally stable bend structures. These structures acquire different cross sections and thus they drift with different velocities in general. However, the trapping of ions within the potential basins at strong fields lasts only for some time before they get excited and move within the intramolecular potential until they get trapped again in the same or different potential minimum due to collision with the gas molecules. Because of this hopping between the potential minima, a portion of the ions has energy above the internal potential barriers affecting the arrival time distributions. This effect increases with the field strength, and its extent can be studied by our MD procedure.

In the following section, we present detailed information about the model molecular ion structure and interactions as well as the main aspects of the employed simulation method. The results of the procedure involving the ion motion and the distribution of ion structures follow in the next section. Finally, in the conclusions, we summarize our predictions and comment about the possibility of using Wannier energy as a parameter for the characterization of the transport and the population of the ion structures at strong electric fields.

## 2. METHODS

The motion of ions in low-density gases under the action of an electrostatic field reaches a quasi-equilibrium state through efficient dissipation of the excess ion energy that is acquired due to the action of the field. The ion flux can be described within the usual experimental accuracy by two main contributions,[15] one for the drift motion, $\mathbf{J}_v$, and the other for the diffusion, $\mathbf{J}_d$,

$$\mathbf{J} = \mathbf{J}_v + \mathbf{J}_d \quad (2)$$

here, $\mathbf{J}_v = n\mathbf{v}$ and $\mathbf{J}_d = -\mathbf{D}\nabla n$, where $n$ and $\mathbf{v}$ are the density and velocity of the ions and $\mathbf{D}$ is the diffusion coefficient. This coefficient at strong fields becomes a two-dimensional matrix with only diagonal elements and two independent components $D_{XX} = D_{YY}$ and $D_{ZZ}$ assuming the field is in the $z$-direction.

At the molecular level, the ions during their flight accumulate translational and internal energies above the equilibrium values and their distributions deviate from the canonical form of equilibrium, as has been observed experimentally[17,18] and reproduced through the solution of the Boltzmann kinetic equation and its generalizations applied for the ions.[19,20] In addition, nonequilibrium Monte Carlo[21−23] and MD simulations[4,13,24−27] have been employed for the calculation and prediction of ion properties, the latter being more easily implemented in the case of molecular systems. So far, the reproduction of the motion of the ions involving internal excitation in strong fields through the use of the analytic theory has not been attempted except in the case of rigid diatomic ions.[28] Internal excitation of molecular ions can be studied straightforwardly by molecular dynamics simulations since particle trajectories (or wave functions) are calculated in time without the use of predetermined (many-coordinate) cross sections, although at the cost of high amounts of computer time.[4,13]

Although the MD simulation methods are powerful in providing the molecular ion properties with the use of proper ion-neutral interactions, the analytic theory usually in its low order of approximation provides relations that are useful in analyzing and organizing the experimental data.[15,29−31] One such expression relates the ion mobility, $K = v_d/E$, with the field strength $E$, to the ion-neutral interaction potential via a collision cross section $\Omega^{1,1}$:[15]

$$K = \frac{3Ze}{16N}\left(\frac{2\pi}{\mu kT_{eff}}\right)^{1/2}\frac{1+\alpha}{\Omega^{1,1}} \quad (3)$$

where Ze is the ion charge, $N$ is the gas number density, $\mu$ is the reduced mass, $T_{eff}$ is given by eq 1, and $\alpha$ is a small parameter that contributes about 2% at strong fields in the large ion limit. In traditional IMS weak-field experiments, $T_{eff}$ is set equal to $T$, $\alpha$ is neglected, and $\Omega^{1,1}$ is replaced by an effective quantity $\Omega$,[32] which is approximated through trajectory simulations based on numerically designed molecular structures.[33,34] The above equation is used in IMS analysis in reverse order, that is, for the determination of the ion molecular structure from the estimated ion-neutral cross section and the measured drift velocity.

Here, we employ a molecular dynamics method developed before[13] for the simulation of the motion of a flexible large ion. The molecular structure of the ion consists of two stiff cylindrical bodies of length $L$ forming an angle ($\varphi$) that changes in time, accommodating part of the internal energy. In the procedure, the ions move in space independent of one another with periodic boundary conditions influenced by the electric field and interacting with "images" of neutral species. These images are selected from an equilibrated MD procedure for the gas molecules.[4,25] Except for the motion of the center of



DOI: 10.1021/acs.jpca.9b03441
J. Phys. Chem. A 2019, 123, 5683−5691

mass (CM) of the ion, which follows Newton's law, the rotation follows Euler's equations with $\varphi$-dependent moments of inertia, $I_{ii}$, expressed through the moments of a (single) cylindrical rigid body about its symmetry axes, $I^c_{ii}$ (with $i = z$ along the cylinder axis)

$$I_{xx} = 2I^c_{xx} + m\sigma_o^2$$
$$I_{yy} = 2\cos^2\frac{\varphi}{2}I^c_{yy} + 2\sin^2\frac{\varphi}{2}I^c_{zz}$$
$$I_{zz} = 2\cos^2\frac{\varphi}{2}I^c_{zz} + 2\sin^2\frac{\varphi}{2}I^c_{yy} + m\sigma_0^2 \quad (4)$$

where $z$ is the main symmetry axis and $x$ the axis perpendicular to the symmetry plane that intersects both cylinders of the ion, and $\sigma_0$ is the distance between the CMs of a cylinder and the molecule. Finally, the moments of inertia of a cylinder of radius $R$ and length $L$ are $I^c_{xx} = I^c_{yy} = \frac{m_c}{4}(R^2 + L^2/3)$ and $I^c_{zz} = \frac{m_c}{2}R^2$, with the mass of a cylindrical body $m_c = m/2$. The vibration depends on the kinetic energy, which is determined through the following equation

$$E_\varphi = \frac{1}{2}I_\varphi\dot{\phi}^2 \quad (5)$$

with $I_\varphi = \frac{1}{4}(2I^c_{xx} + m\gamma^2)$ being the moment of inertia for the angular motion of $\varphi$ and $\gamma$ the distance of the CM from the bending point. With the momentum for the angular motion $p_\varphi = I_\varphi\dot{\varphi}$, the equations of motion for the molecular angle are obtained from the Hamiltonian

$$H_\varphi = \frac{L_x^2}{2I_{xx}} + \frac{L_y^2}{2I_{yy}} + \frac{L_z^2}{2I_{zz}} + \frac{p_\varphi^2}{2I_\varphi} + V(\varphi) + V_{ext} \quad (6)$$

where $V(\varphi)$ is the intramolecular potential and $V_{ext}$ the potential due to the interacting gas molecules and the external electric field.

The trajectories of the consecutive ion-neutral encounters are accumulated and used for the calculation of the ion molecular properties. Thus, the drift velocity is determined through the velocity average $v_d = \langle v_z\rangle$, from which the ion mobility, $K = v_d/E$, is calculated. The translational energy in the $i$-direction (with $i$ being $X$, $Y$, $Z$) is obtained from the equation

$$E_i = \frac{m}{2}\langle v_i^2\rangle, \text{ with } E_X \approx E_Y \quad (7)$$

and the rotational energy around the $i$-axis is calculated from $E_{ri} = \frac{1}{2}\langle I_{ii}\omega_i^2\rangle$, where $\omega_i$ is the corresponding angular velocity in the body frame. Further, the angular kinetic energy is calculated from eq 5. The method provides additionally angle and velocity distributions, distribution of residence times at intramolecular potential minima, and time-dependent velocity correlation functions of a component $i$, $C_{ii} = \langle(v_i(0) - \langle v_i(0)\rangle)(v_i(t) - \langle v_i(t)\rangle)\rangle$, from which the corresponding diffusion component can be calculated through the following equation

$$D_{ii} = \int_0^\infty C_{ii}(t)\mathrm{d}t \quad (8)$$

Since $C_{XX} = C_{YY}$, two independent diffusion components are obtained: $D_\perp = (D_{XX} + D_{YY})/2$ and $D_\parallel = D_{ZZ}$.

Following our previously developed approach, the molecular structures of the ions are introduced through an intramolecular potential that depends on the ion angle, $V(\varphi)$.[13] Depending on the position and depth of the potential minima, the relative population of the structures is expected to vary with the gas temperature and the electric field strength since both these operational parameters control the relative ion-neutral collision energy (eq 1). As will be seen below, the ion dynamics perplexes this simple picture and the population of the structures deviates from the normal equilibrium distribution. The relaxed quasi-equilibrium composition of the structures and the detailed ion motion depend on the specific ion-neutral interactions and cannot be predicted in advance, especially since the rotation and angular vibration of the ions are coupled and both are influenced directly by the action of the external field.

Although our approach is general, by way of an example, we consider the structure of BIP ions,[10] by introducing three minima in the angular potential (Figure 1). The angular potential, $V_{n,m}(\varphi)$, is constructed by two polynomial functions and two Gaussians with parameters presented in Table 1

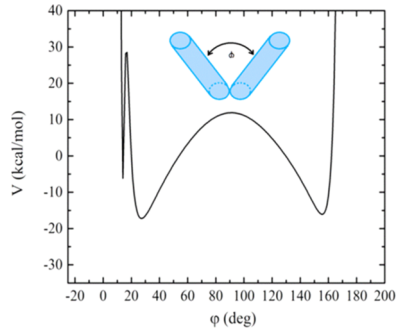


**Figure 1.** Angular intramolecular potential with three minima at very small (13.88°), small (27.19°), and large (156.6°) angles.

$$V_{n,m}(\varphi) = \sum_{i=1,2}(V^i_{n,m}(\varphi) + V^i_G(\varphi)) \quad (9)$$

**Table 1. Angular Potential Parameters**

| | $\varphi_{m,i}$ (deg) | $\varphi_{0,i}$ (deg) | $\varepsilon_i$ (kcal/mol) | $A_i$ (kcal/mol) | $\sigma_i$ (deg) |
|---|---|---|---|---|---|
| $V^1_{4,2}(\varphi)$ | 28 | | 20 | | |
| $V^2_{4,2}(\varphi)$ | 156 | | 18 | | |
| $V^1_G(\varphi)$ | | 90 | | 16 | 35 |
| $V^2_G(\varphi)$ | | 12.6 | | −10.2 | 1.8 |

with

$$V^i_{n,m}(\varphi) = \frac{n\varepsilon_i}{n-m}\left[\frac{m}{n}\left(\frac{\varphi_{n,i} - \alpha_i}{\varphi - \alpha_i}\right)^n - \left(\frac{\varphi_{m,i} - \alpha_i}{\varphi - \alpha_i}\right)^m\right] \quad (10)$$

using $n = 4$, $m = 2$, $\alpha_1 = 0°$, $\alpha_2 = 180°$, and

$$V^i_G(\varphi) = \frac{A_i}{\sigma_i\sqrt{2\pi}}\exp[-(\varphi-\varphi_{0,i})^2/2\sigma_i^2] \quad (11)$$

The compact structure is located at a very small angle of 13.88° and −6.153 kcal/mol depth, relative to the asymptote of the potential of eq 10, with a large potential barrier of 36.44 kcal/mol from the side of the compact structure, which is difficult to be crossed (Figure 1). The other two minima,


DOI: 10.1021/acs.jpca.9b03441
J. Phys. Chem. A 2019, 123, 5683−5691

corresponding to a closed and an open isomer, have similar depths of −17.16 and −16.23 kcal/mol at 27.19 and 156.6°, respectively, with a barrier between them of 28.33 kcal/mol from the side of the open structure. The height of this barrier is appropriate to obtain adequate structure interchanges as they appear in the excitation region of IMS and is close to the experimental value of 28.66 kcal/mol.[10]

The interaction of the ion with the neutral gas, which here is $N_2$, is described by a 12-6-4 polynomial potential that acquires the right polarization term at long distance

$$V(r) = \frac{\varepsilon_0}{2}\left[(1+\gamma)\left(\frac{r_m}{r}\right)^{12} - 4\gamma\left(\frac{r_m}{r}\right)^{6} - 3(1-\gamma)\left(\frac{r_m}{r}\right)^{4}\right] \quad (12)$$

where $\gamma$ is estimated by setting the last term equal to the first term of the ion-neutral induction series expression

$$\frac{3\varepsilon_0}{2}(1-\gamma)\left(\frac{r_m}{r}\right)^4 = \frac{e^2 a_d}{2r^4} \quad (13)$$

With the dipole polarizability $a_d$ = 1.74 Å$^3$ for $N_2$ as well as $r_m$ = 4.27 Å and $\varepsilon_0$ = 0.65 kcal/mol for the position and the depth of the interaction potential, respectively, the $\gamma$ parameter is found to be 0.8678. The strength of the interaction has been determined following the approach of Cambi et al.[35] and subsequent calibration to produce reasonable populations for the ion structures. The force on the ion is assumed to be applied perpendicular to the axis of the cylindrical bodies and at a distance of 1.34 Å. The rotational motion is controlled by the components of the angular momentum, which are calculated in the body frame by setting the length of the cylinders equal to $L$ = 4.5 Å. For the gas interactions, we employ a standard Lennard-Jones potential with $\varepsilon_0$ = 0.189 kcal/mol and $r_m$ = 3.698 Å,[36] which is efficient for the calculations and reproduces well the properties of $N_2$ under low-density conditions. We mention that the exact gas potential is not crucial for the determination of the ion motion under ideal gas conditions and that the vibration of $N_2$ is not expected to be excited under the experimental conditions and the conditions considered here. Although most of the excitation of the ions emerges from the encounter with the neutrals, the external field influences directly both the rotation and the vibration rather weakly, depending on the position of the charge on the molecular structure. Here, we consider a static charge located at the end of one of the arms of the ion. Examination of the results with the charge at the CM has shown small changes, such as 1% in the mobility and a few percents in the effective ion temperatures and the structure population at $T$ = 150 K and $E/N$ = 50 Td. At high field strengths, however, a thorough study is required for the examination of the effect of the charge location on the ion motion.

## 3. RESULTS

There are four stages in the simulation procedure. First, the gas is equilibrated under microcanonical conditions constrained at a certain temperature and then left to evolve without temperature control. Subsequently, the ions are forced to acquire predetermined values for the velocity, the mean translational kinetic energies parallel and perpendicular to the field, and the rotational energy. At the third stage, the ions are left to relax at their final steady motion without external control. Despite the continuous acceleration of the ions by the field, no need for temperature control is required because they interact efficiently with cooler images of neutrals that extract the surplus of their energy.[13] At the last stage, mean values of the dynamic variables are calculated periodically (locally) for the monitoring of the ion motion. This is necessary, especially at high fields where the ion energy may not be dissipated efficiently during the ion-neutral collisions, and runaway events could occur. However, occasionally, even at lower field strengths, individual ions may acquire high velocities that persist long enough to deteriorate the accuracy of the statistical calculations. Such events are monitored and excluded from the calculations. At the end of the procedure, the global averages of the distributions and their moments are calculated.

We implement our computer code[13] in parallel using 130 (independent) ions in 108 $N_2$ molecules, with the molar volume fixed at 0.02 m$^3$, at various gas temperatures and field strengths. We have found that 40 processes are the most efficient in providing around $5 \times 10^7$ collision events, with each process running for 5 ns with a time step of 0.1 fs.

**3.1. Relaxation and Rotational Alignment.** During the simulation, the velocity relaxes first, then the second moments of the velocity distribution (or kinetic energies) follow, and lastly the angular distribution reaches a quasi-equilibrium form, where the locally stable structures convert one to another at the same rate. The molecular interchanges are rare at low ion-neutral energies and difficult to sample through molecular simulations, but increase considerably at high collision energies.

The angular relaxation of the large ion, starting from a homogeneous initial angular distribution, is followed through the time variation of the mean (local) bending angle as seen in Figure 2 for different gas temperatures and field strengths.

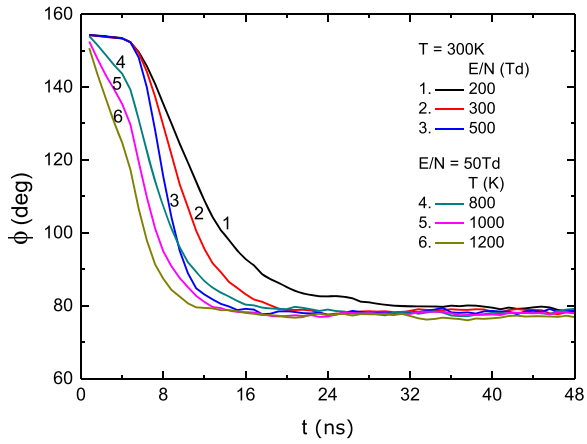


**Figure 2.** Relaxation of the mean angle of ions toward limiting values for different cases; 1−3 at $T$ = 300 K with a variable field strength, and 4−6 with 50 Td at various high temperatures.

At the relaxed stage, the ions are found to align relative to the $z$-direction of the electric field so that the angular momentum in the direction perpendicular to the field is larger than that parallel to it. This difference increases with the field, as seen in Figure 3, where the quadrupole alignment parameter[37] $A_0^{(2)} = 3\langle L_z^2\rangle/\langle L_x^2 + L_y^2 + L_z^2\rangle - 1$ decreases with respect to the Wannier effective temperature, implying stronger alignment. However, the parameter appears to vanish at weak fields, such as 50 Td, as the gas temperature is increasing (upper curve), indicating $\langle L_x^2\rangle = \langle L_y^2\rangle = \langle L_z^2\rangle$. In this


DOI: 10.1021/acs.jpca.9b03441
J. Phys. Chem. A 2019, 123, 5683−5691

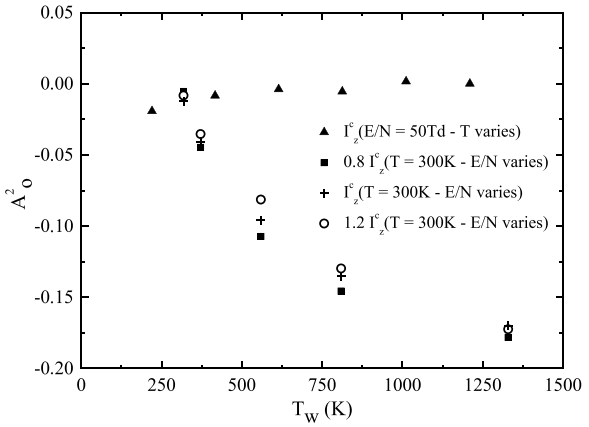


**Figure 3.** Quadrupole alignment parameter, $A_0^{(2)}$, with respect to $T_w = 2E_w/3k$ at $T$ = 300 K and a variable field strength for three different moments of inertia; squares represent 0.8 $I^c_{zz}$, crosses $I^c_{zz}$, and circles 1.2 $I^c_{zz}$. Cases of the same field and different temperatures are represented by triangles.

case, the field effect diminishes relative to the randomization of the ion motion through the collisions with the hot gas molecules. Persistence of the rotational alignment is observed in heavier ions with the $A_0^{(2)}$ parameter decreasing with respect to the ion mass. Analogous ion rotation alignment has been observed from similar MD simulations for smaller molecules such as $NO^+$ and $H_2O^+$ at strong fields with the "helicopter"-type motion prevailing relative to the "airplane" one.[27]

**3.2. Mobility and Energies.** To examine the use of the Wannier (relative collision) energy as a parameter for the characterization of the nonequilibrium states of the ions, we first plot the standard mobility, $K_0$, with respect to the effective temperature, $T_w$, for two main cases: one involving the system at two gas temperatures ($T$ = 150 and 300 K) for a range of field strengths and another at one field strength ($E/N$ = 50 Td) and various gas temperatures (Figure 4). We observe the results of all cases to remain close to each other, with the two systems of different field strengths not differing by more than 2%. The case of constant field strength (and variable temperature) follows closely, by about ±5%, even at large

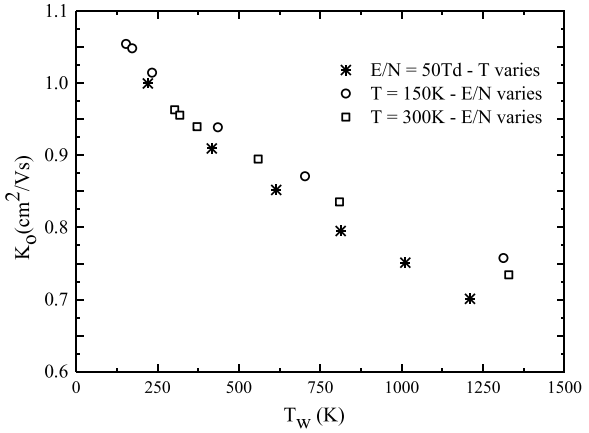


**Figure 4.** Ion mobility for three different cases; stars represent a constant field strength, $E/N$ 50 Td, with a variable temperature, and circles and squares represent a variable field strength and constant temperatures of 150 and 300 K, respectively.

temperature values. We mention that in the latter cases, the ions remain rather close to equilibrium since $E/N$ is 50 Td.

The kinetic energy contributions of all velocity components of translation and rotation, as plotted in Figure 5, seem to

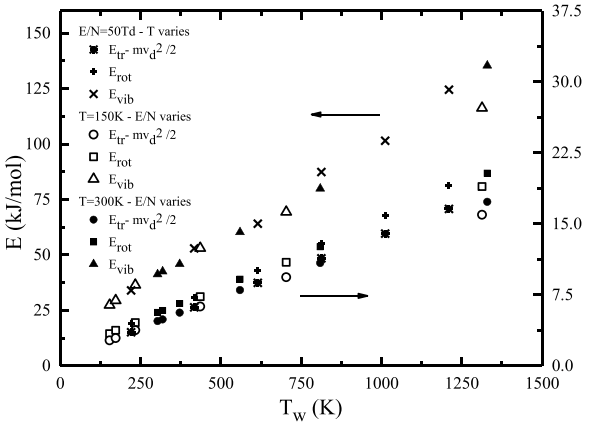


**Figure 5.** Ion translation, rotation, and (kinetic) vibration energy contributions for three different cases; line symbols represent a constant field and variable temperature, and geometric symbols represent a constant temperature and variable field strength at 150 and 300 K, respectively.

group together as functions of $T_w$. The $y$-component of the rotational energy, along the axis that intersects the CM of the two cylindrical bodies of the ion (not shown), has been found to exceed the $x$ and $z$ components. This effect is sensitive to the intramolecular potential and is found to decrease with the increase of the depth of the potential minimum of the closed form. The angular vibration, however, appears to differ and be excited more than the rest of the degrees of freedom, although the vibration energies of all different cases still follow a single curve. Repeating the simulations with various ion and gas masses, we observe that the ion vibration energy approaches the energy of the rest of the degrees of freedom when the ion mass becomes quite larger than the mass of the neutral, $m \gg M$. In this case, the energy that emerges during the ion-neutral encounter of the ions with the neutrals appears more difficult to be accumulated in the angular vibration of the ion.

By modifying the extension of the ion, assuming that the molecular mass is equally distributed, we examine the effect of the rotation on the motion of the ion. For the two new volumes of 0.6 and 1.4 times the original volume of the ion, leading to moments of inertia 0.8 and 1.2 times the original one, we observe a considerable variation of the standard mobility, with the ions of the smaller moment of inertia traveling faster through the neutral gas (Figure 6). The corresponding relative alignment of the angular momentum as seen in Figure 3, however, changed less drastically.

**3.3. Bending Structure Distributions.** The relaxed joint angle−$v_z$ distributions vary considerably with the relative collision energy between the ions and the gas molecules (Figure 7). We observe peaks related to the dominant open and closed structures with potential minima at 27.19° and 156.6°, respectively. The compact structure with a potential minimum at 13.88° is populated only at high relative collision energies and its contribution to the transport remains quite small. At certain gas temperatures, for example at $T$ = 300 K, as the field strength increases, the distribution shifts to a higher $v_z$ velocity component and changes form. At low field strengths,



DOI: 10.1021/acs.jpca.9b03441
J. Phys. Chem. A 2019, 123, 5683−5691

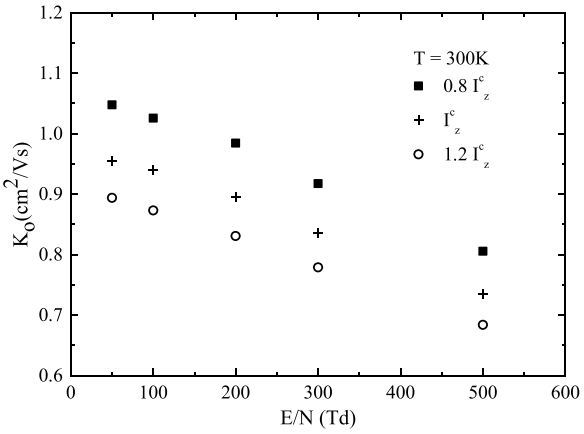


**Figure 6.** Mobility of ions with different moments of inertia at various field strengths. $I_z^c$ is the original moment of inertia entering in eq 4.

the open structure is dominant and at stronger (intermediate) fields some probability is transferred from the open to the closed isomer, whereas at high field strengths, the population of both main structures seems to diminish. This occurs because the intermediate angular region is populated, indicating that a considerable portion of the molecular ions vibrates over the entire angular range. At this excitation regime, the compact structure, below 15°, starts to acquire population (Figure 8).

The relaxed relative population of the structures can be estimated from the angular distributions, irrespective of the velocity, such as those of Figure 8, by integrating the probability density within the angular regions defined by the maxima of the intramolecular potential of Figure 1. The calculations, since they count the number of ions that are found in specific angular regions, can be associated with measured populations whenever the excited ions are relaxed and trapped at the potential basins during their travel through the experimental apparatus. It is in this sense that the calculated populations can be compared with the IMS−IMS measurements, where a long drift tube of normal temperature and weak electric field is placed after the excitation region.

The resulting populations of the three molecular structures for the two types of conditions (constant temperature at different field strengths and vice-versa described above) are found to follow the same curves as functions of $T_w$ (Figure 9). Irrespective of the applied conditions the Wannier energy is found to express in a unifying manner the populations of the ion structures of the present system. The form of the curves, however, is system-dependent and, at low effective temperatures, the populations are sensitive to the dynamics. Although the coupling between vibration and rotation affects weakly the ion mean motion, the rotation energy acts as an effective potential to the vibration (eq 6), modifying the relative depths of the angular potential as shown in Figure 1. The additional direct effect of the external field on the rotation and vibration, since the ions are pulled from one end of the molecular structure, is found not to alter significantly the structures of the ions.

Further, we have studied the sensitivity of the results on the angular potential, the ion mass, and the moments of inertia. A drastic change occurs with the deepening of the second minimum of the potential by 4.9 kcal/mol ($\varepsilon_1$ = 25 kcal/mol) and 13 kcal/mol ($\varepsilon_1$ = 30 kcal/mol). The relative population of the second to the third structures was inverted at weak fields ($E/N$ = 50 Td and 150 K) and, instead of the initial ratio of

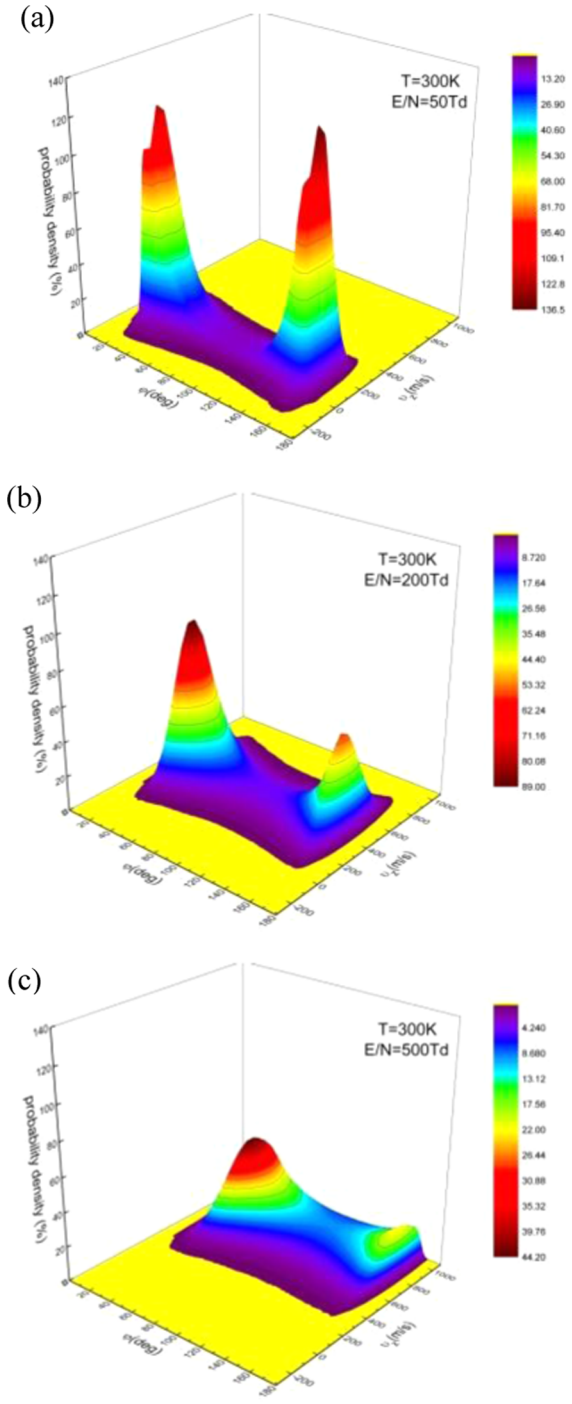


**Figure 7.** Joint angle−$v_z$ distribution at 300 K and three different field strengths, increasing from (a) to (c).

0.70, we obtained the values of 0.85 and 1.03, with respect to the depth of the potential. This sensitivity vanishes at strong fields, since under these conditions the closed (second) structure dominates over the open (third) one, and all potentials attain the same limit (Figure 9). A similar behavior was observed when the mass of the ion was increased to eight times the original mass at a weak field of 5 Td at 150 K. In this case, the attained percent populations, 0.0, 59.5, and 40.5, for the three ion structures appear to be normal for a system with small vibration excitation as presented above ($m \gg M$).



DOI: 10.1021/acs.jpca.9b03441
J. Phys. Chem. A 2019, 123, 5683−5691

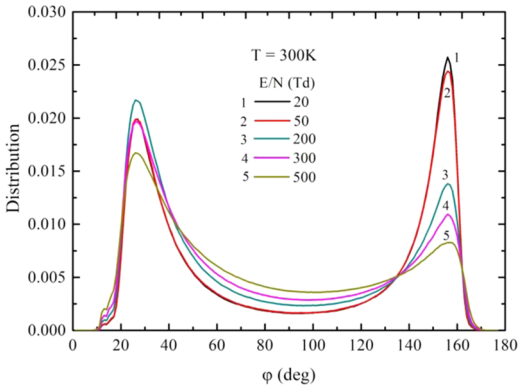


**Figure 8.** Distribution of angles at $T$ = 300 K and various field strengths.

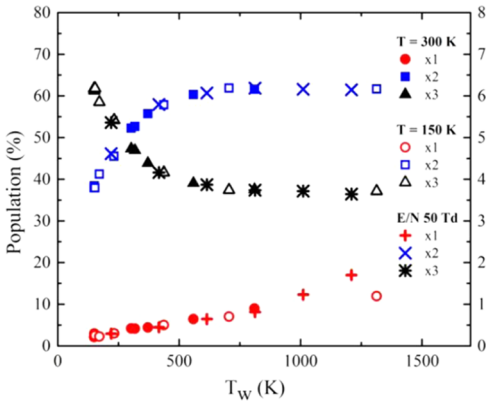


**Figure 9.** Population of ion structures with respect to the effective temperature $T_w$. The parameters $x_1$, $x_2$, and $x_3$ correspond to structures with potential minima at very small, small, and large angles, respectively. The $x_1$ parameter is measured through the right scale.

The effect of rotation on the distribution of the structures is observed through the use of components of the moments of inertia of twice or half the size of the ones of the model system. By varying $I^c_{zz}$, using compatible $I^c_{xx}$ and $I^c_{yy}$ components, we observe an increase of the population of the open structure relative to the closed one as the moments of inertia increase. Although this result is in the same direction of the mass effect, it appears to be quite weaker without inversion of the initial population at weak fields.

A comparison of the results with the IMS measurements for the BIP ions[10] is attempted only at high field strengths since the experimental ion structures relax to quasi-equilibrium distributions at ambient gas temperatures only at strong fields and simulations produce converged results again at aged systems. The obtained relative (relaxed) distribution of dominant structures is about 62% for the open and 37% for the closed structure, in conformity to the experimental result for the observed main structures, which are estimated to be 57% for the cis and 39% for the trans conformations, respectively. Further, the population of the third compact structure is found to be 1 order of magnitude smaller than that in the IMS measurements.

The results are sensitive to the intramolecular and ion-neutral potentials and can be modified by changing them; however, the emergence of single curves in the population graph of Figure 9 should be a general indication that the collision excitation due to the field resembles the one caused by the temperature increase alone, at least for the case of large ion systems. The introduction, however, of the latter excitation procedure in IMS measurements would require a different, possibly more difficult, experimental design.

## 4. CONCLUSIONS

Mobility measurements of large flexible ions provide information about the distribution of possible conformations of molecular structures that emerge from collision excitation. Such situations arise in ion mobility measurements where ions move in gases under the action of an electrostatic field. Excitation of ion internal motion can take place at a high gas temperature or at strong fields, due to the increase of the relative ion−gas collision energy and transfer of a part of the energy to the internal degrees of freedom of the ion. However, there is a difference in the action of the two operational parameters of the system. As the gas temperature is increased at weak fields, the velocity, angular velocity, and vibration distributions acquire a universal equilibrium form, although at high field strengths, the distributions attain nonequilibrium forms that are system-dependent.

The two modes of excitation have been compared through the use of a nonequilibrium molecular dynamics method for the simulation of the ion motion, which we have developed in the past. We mention that the field effect on the translation and rotation of "rigid" molecular ions has been studied thoroughly in the past. Here, we have employed an intramolecular potential that determines the ion−molecular metastable structures as well as appropriate ion−gas and gas−gas interaction potentials for the MD simulation of the ion motion. With these provisions during the simulation, the ions continuously translate, rotate, and vibrate as they move in a structureless gas. The molecular properties of the ions have been matched as closely as possible to the BIP ion, which has been employed in IMS measurements, and the relative populations of the stable structures have been probed for a number of field strengths at certain gas temperatures. Although a few different but similar molecular (BIP) ions may be involved in the experiment, here we have considered appropriate interactions and a single ion type with three relatively stable structures to reproduce effectively the experimental results.

At the wide range of the studied field strengths, we found that the translation and the rotation energies follow closely the mean collision energy as described by the Wannier energy expression. However, as the field strength is increased at ambient gas temperatures, the ions align so that the angular momentum perpendicular to the field is larger than the one parallel to it. This effect has occurred in the past with smaller ions and denotes that ions move more efficiently through the gas with the helicopter-type motion than with the airplane motion. The opposite happens as the gas temperature increases at weak fields, since the randomization of the ion rotation due to the gas motion prevails. The vibration energies also follow a unique curve with respect to $T_w$, but at higher values than $E_w$. This effect occurs at high fields but diminishes as the ratio of the ion to neutral mass is increased. The explanation of the deviation of the vibrational kinetic energy from $E_w$, in the case of relatively small ions, requires further study.

The angular distributions of the ions are not affected significantly at high field strengths contrary to what would be expected due to the rotational alignment and the coupling between the rotation and the vibration. Still, the two modes of



DOI: 10.1021/acs.jpca.9b03441
J. Phys. Chem. A 2019, 123, 5683−5691

excitation produce populations that arrange themselves in unique curves in terms of $T_w$, irrespective of the ions being close to equilibrium (variable temperature) or away from equilibrium (variable field strength). The comparison of the calculated structure distributions of the employed molecular system against experimental populations, which have been obtained through electric field excitation in a narrow region in the middle of an IMS−IMS apparatus, has shown that the present procedure can reproduce the vibrational motion of the ions at strong fields.

The present method has been implemented for the reproduction of the mean motion, dynamics, and population of the conformations of the ions primarily at strong electric fields based on the molecular bending structure of the ion and the ion-neutral interactions. Here, we have examined the case of large ions in a lighter gas molecule, whereas the examination of the behavior of smaller molecular ions with angular degrees of freedom away from equilibrium should be studied further.

## AUTHOR INFORMATION


### Corresponding Author

*E-mail: akoutsel@chem.uoa.gr. Tel: +30-210-7274536.

### ORCID

Andreas D. Koutselos: 0000-0003-4031-0559


### Notes

The authors declare no competing financial interest.

## ACKNOWLEDGMENTS

This work was supported by the Special Research Account of the National and Kapodistrian University of Athens. Computational time was granted by the Greek Research & Technology Network (GRNET) in the National HPC facility ARIS under project pr004017-FLEXPEPT. The authors would like to thank Dr D. Dellis for his advice related to the application of our code in the ARIS supercomputer.

## REFERENCES


(1) Bastian, M. J.; Lauenstein, C. P.; Bierbaum, V. M.; Leone, S. R. Single frequency laser probing of velocity component correlations and transport properties of Ba + drifting in Ar. *J. Chem. Phys.* **1993**, *98*, 9496−9512.

(2) Anthony, E. B.; Schade, W.; Bastian, M. J.; Bierbaum, V. M.; Leone, S. R. Laser probing of velocity-subgroup dependent rotational alignment of $N_2^+$ drifted in He. *J. Chem. Phys.* **1997**, *106*, 5413−5422.

(3) Mason, E. A.; McDaniel, E. W. *Transport Properties of Ions in Gases*; Wiley: New York, 1988; p 31.

(4) Koutselos, A. D. Ion dynamics in electrostatic fields. *J. Phys. B: At., Mol. Opt. Phys.* **1999**, *32*, 1225−1231.

(5) Koeniger, S. L.; Merenbloom, S. I.; Valentine, S. J.; Jarrold, M. F.; Udseth, H. R.; Smith, R. D.; Clemmer, D. E. An IMS−IMS analogue of MS−MS. *Anal. Chem.* **2006**, *78*, 4161−4174.

(6) Zilch, L. W.; Kaleta, D. T.; Kohtani, M.; Krishnan, R.; Jarrold, M. F. Folding and unfolding of helix-turn-helix motifs in the gas phase. *J. Am. Soc. Mass Spectrom.* **2007**, *18*, 1239−1248.

(7) Urner, L. H.; Thota, B. N. S.; Nachtigall, O.; Warnke, S.; von Helden, G.; Haag, R.; Pagel, K. Online monitoring the isomerization of an azobenzene-based dendritic bolaamphiphile using ion mobility-mass spectrometry. *Chem. Commun.* **2015**, *51*, 8801−8004.

(8) Scholz, M. S.; Bull, J. N.; Coughlan, N. J. A.; Carrascosa, E.; Adamson, B. D.; Bieske, E. J. Photoisomerization of protonated azobenzenes in the gas phase. *J. Phys. Chem. A* **2017**, *121*, 6413−6419.

(9) Bull, J. N.; Carrascosa, E.; Mallo, N.; Scholz, M. S.; da Silva, G.; Beves, J. E.; Bieske, E. J. Photoswitching an isolated donor−acceptor stenhouse adduct. *J. Phys. Chem. Lett.* **2018**, *9*, 665−671.

(10) Coughlan, N. J. A.; Scholz, M. S.; Hansen, C. S.; Trevitt, A. J.; Adamson, B. D.; Bieske, E. J. Photo and collision induced isomerization of a cyclic retinal derivative: An ion mobility study. *J. Am. Soc. Mass Spectrom.* **2016**, *27*, 1483−1490.

(11) Pierson, N. A.; Clemmer, D. E. An IMS−IMS threshold method for semi-quantitative determination of activation barriers: Interconversion of proline *cis* ↔ *trans* forms in triply protonated bradykinin. *Int. J. Mass Spectrom.* **2015**, *377*, 646−654.

(12) Dilger, J.; Musbat, L.; Sheves, M.; Bochenkova, A. V.; Clemmer, D. E.; Toker, Y. Direct measurement of the isomerization barrier of the isolated retinal chromophore. *Angew. Chem., Int. Ed.* **2015**, *54*, 4748−4752.

(13) Litinas, I.; Koutselos, A. D. Molecular dynamics simulation for the dynamics and kinetics of folding peptides in the gas phase. *J. Phys. Chem. A* **2015**, *119*, 12935−12944.

(14) Gidden, J.; Wyttenbach, T.; Jackson, A. T.; Scrivens, J. H.; Bowers, M. T. Gas-phase conformations of synthetic polymers: poly(ethylene glycol), poly(propylene glycol), and poly-(tetramethylene glycol). *J. Am. Chem. Soc.* **2000**, *122*, 4692−4699.

(15) Mason, E. A.; McDaniel, E. W. *Transport Properties of Ions in Gases*; Wiley: New York, 1988.

(16) Wannier, G. H. Motion of gaseous ions in strong electrostatic fields. *Bell Syst. Tech. J.* **1953**, *32*, 170−254.

(17) Dressler, R. A.; Beijers, J. P. M.; Meyer, H.; Penn, S. M.; Bierbaum, V. M.; Leone, S. R. Laser probing of ion velocity distributions in drift fields: Parallel and perpendicular temperatures and mobility for Ba + in He. *J. Chem. Phys.* **1988**, *89*, 4707−4715.

(18) Penn, S. M.; Beijers, J. P. M.; Dressler, R. A.; Bierbaum, V. M.; Leone, S. R. Laser-induced fluorescence measurements of drift-velocity distributions for $Ba^+$ in Ar: Moment analysis and a direct measure of skewness. *J. Chem. Phys.* **1990**, *93*, 5118−5127.

(19) Viehland, L. A. Velocity distribution functions and transport coefficients of atomic ions in atomic gases by a Gram-Charlier approach. *Chem. Phys.* **1994**, *179*, 71−92.

(20) Ness, K.; Viehland, L. A. Distribution functions and transport coefficients for atomic ions in dilute gases. *Chem. Phys.* **1990**, *148*, 255−275.

(21) Skullerud, H. R. Monte-Carlo investigations of the motion of gaseous ions in electrostatic fields. *J. Phys. B: At. Mol. Phys.* **1973**, *6*, 728−742.

(22) Lin, S. L.; Bardsley, J. N. Monte Carlo simulation of ion motion in drift tubes. *J. Chem. Phys.* **1977**, *66*, 435−445.

(23) Ong, P. P.; Hogan, M. J.; Lam, K. Y.; Viehland, L. A. Interaction potential, transport properties, and velocity distributions of Na+ ions in Ne. *Phys. Rev. A* **1992**, *45*, 3997−4009.

(24) Koutselos, A. D. Molecular dynamics simulation of gaseous ion-motion in electrostatic fields. *J. Chem. Phys.* **1995**, *102*, 7216−7220.

(25) Balla, G.; Koutselos, A. D. Molecular dynamics simulation of ion transport in moderately dense gases in an electrostatic field. *J. Chem. Phys.* **2003**, *119*, 11374−11379.

(26) Baranowski, R.; Wagner, B.; Thachuck, M. Molecular dynamics study of the collision-induced rotational alignment of $N_2^+$ drifting in helium. *J. Chem. Phys.* **2001**, *114*, 6662−6671.

(27) Chen, X.; Thachuck, M. Collision-induced alignment of $H_2O^+$ drifting in helium. *J. Chem. Phys.* **2006**, *124*, 174501−174508.

(28) Viehland, L. A.; Dickinson, A. S. Transport of diatomic ions in atomic gases. *Chem. Phys.* **1995**, *193*, 255−286.

(29) Waldman, M.; Mason, E. A. Generalized Einstein relations from a three-temperature theory of gaseous ion transport. *Chem. Phys.* **1981**, *58*, 121−144.

(30) Koutselos, A. D.; Mason, E. A. Generalized Einstein relations for ions in molecular gases. *Chem. Phys.* **1991**, *153*, 351−370.

(31) Viehland, L. A.; Mason, E. A. Transport properties of gaseous ions over a wide energy range, IV. *At. Data Nucl. Data Tables* **1995**, *60*, 37−95.

(32) Mason, E. A. *Plasma Chromatography*; Carr, T. W., Ed.; Plenum: New York, 1984; p 43.




DOI: 10.1021/acs.jpca.9b03441
J. Phys. Chem. A 2019, 123, 5683−5691

(33) Bohrer, B. C.; Merenbloom, S. I.; Koeniger, S. L.; Hilderbrand, A. E.; Clemmer, D. E. Biomolecule analysis by ion mobility spectrometry. *Annu. Rev. Anal. Chem.* **2008**, *1*, 293−397.
(34) Wyttenbach, T.; Pierson, N. A.; Clemmer, D. E.; Bowers, M. T. Ion mobility analysis of molecular dynamics. *Annu. Rev. Phys. Chem.* **2014**, *65*, 175−196.
(35) Cambi, R.; Cappelletti, D.; Liuti, G.; Pirani, F. Generalized correlations in terms of polarizability for van der Waals interaction potential parameter calculations. *J. Chem. Phys.* **1991**, *95*, 1852−1861.
(36) Hirschfelder, J. O.; Curtiss, C. F. *Molecular Theory of Gases and Liquids*; John Wiley: New York, 1964, Appendix I.
(37) Orr-Ewing, A. J.; Zare, R. N. Orientation and alignment of reaction products. *Annu. Rev. Phys. Chem.* **1994**, *45*, 315−366.



DOI: 10.1021/acs.jpca.9b03441
*J. Phys. Chem. A* 2019, 123, 5683−5691